

# An Analytical Hybrid Model for the Shielding Effectiveness Evaluation of a Dual-Cavity Structure with an Aperture Array

Hai Jin<sup>1, 2</sup>, Hongliang Zhang<sup>1, 2</sup>, Yurun Ma<sup>1, 2, \*</sup>, Kejian Chen<sup>1, 2</sup>, and Xinfeng Sun<sup>3</sup>

**Abstract**—Rectangular dual-cavity structure is usually used to improve the shielding efficiency of a shielding chamber or to avoid the interference among the internal electronic components of the system. In order to simplify the estimation of the shielding effectiveness for a dual-cavity structure with an aperture array, a hybrid analytical model is proposed based on Robinson's model and Dehkoda's model. In the new model, the enclosure of cavity and the aperture array are equivalent to a short-circuited waveguide and admittance, respectively. Using this hybrid model, shielding effectiveness could be calculated efficiently for a common frequency band. The results of typical examples are compared with simulation examples, and they are in very good agreement. This method provides an analytic solution for designers to speed up the design process of a rectangular dual-cavity structure with an aperture array.

## 1. INTRODUCTION

With the rapid development of the high speed integrated circuits and electronic devices in recent years, shielding cavities are usually constructed to reduce the influence of electromagnetic interference or to avoid the interference among the internal electronic components of the system. Shielding effectiveness (SE) is used to estimate the shielding ability of a shielding enclosure, which is the ratio of the field strength in the presence and the absence of the enclosure for both electric and magnetic fields. SE estimation for an enclosure with apertures is attracting widespread interest in electromagnetic compatibility (EMC) research area. In practical applications, considering the factors such as ventilation and heat dissipation, dual-cavity structure is often used to improve the shielding effect. Numerous researches have been carried out previously for evaluating the SE of the shielding enclosures with apertures, comprising numerical methods and analytical methods.

The study of numerical methods has concentrated on different algorithms, including the method of moments (MoM) [1], transmission-line modeling (TLM) method [2], finite-difference time-domain (FDTD) method [3], Baum-Liu-Tesche (BLT) equation [4–7], and finite-element time-domain (FETD) method [8–10]. It is still difficult for designers to calculate the SE with the methods mentioned above because the modelling is complex and time-consuming, especially where the accuracy is not required strictly. The analytical method was advocated by Bethe for the first time [11], then Robinson et al. proposed equivalent circuit method [12]. In Robinson's method, the box modeled by a short-circuited length of rectangular waveguide, and the aperture was represented by a length of transmission line shorted at ends. The subsequent extended analytical methods are mostly based on Robinson's model. Robinson et al. extended their method to predict the electric and magnetic shielding effectiveness of a rectangular enclosure with one or more apertures in one wall [13]. Thomas et al. improved this method

---

Received 31 March 2020, Accepted 20 May 2020, Scheduled 28 May 2020

\* Corresponding author: Yurun Ma (wysyanab@126.com).

<sup>1</sup> College of Electric Engineering and Information Engineering, Lanzhou University of Technology, 730050, China. <sup>2</sup> Key Laboratory of Gansu Advanced Control for Industrial Processes, Lanzhou University of Technology, Lanzhou 730050, China. <sup>3</sup> National Key Laboratory of Science and Technology on Vacuum Technology and Physics, Lanzhou Institute of Physics, China.

which considered the effects of the loading due to conducting planes or printed circuit board within the enclosure [14]. Konefal et al. have extended Robinson's model to include modes higher than  $TE_{10}$  [15]. Dan et al. also extended this method to make the position of the aperture arbitrary [16]. Dehkhoda et al. presented an efficient analytical and accurate model to predict the shielding effectiveness of a rectangular enclosure with numerous small apertures [17, 18]. Ren et al. simplified an aperture array into a single aperture and applied the waveguide equivalent circuit model to calculate the shielding effectiveness of an enclosure with numerous small apertures [19]. Most of these analytical methods are applicable only in the scenario that the size of the hole is much smaller than the wavelength. There are also lots of researches to approach shielding enclosure problems analytically [20–22]. However, these researches mainly focus on the case of single cavity or dual-cavity structure with rectangle enclosure, and few researchers have addressed the problem of a dual-cavity structure with an aperture array.

In this paper, a hybrid analytical model is carried out based on Robinson's model and Dehkhoda's model to predict the shielding effectiveness of a dual-cavity structure with an aperture array. The enclosure of cavity is equivalent to a short-circuited waveguide, and the aperture array is regarded as admittance. We assume a single mode of propagation ( $TE_{10}$ ) for the simplest model, and the incident wave is plane wave. Additionally, the plane wave is characterized by a voltage source and free-space impedance in the simplified circuit. Using this hybrid model, shielding effectiveness for a common frequency band could be calculated efficiently. The results of typical examples are compared with the simulation results to verify the accuracy of the model. This method has a benefit that it provides an analytic solution, for designers to speed up the design process of a rectangular double cavity with an aperture array.

## 2. A HYBRID MODEL ESTABLISHED

The calculation model diagram of the dual-cavity structure as shown in Figure 1. A rectangular metal shielded cavity with dimensions  $a \times b \times c$  is shown in Figure 1(a). Outer aperture array has a dimension  $l_1 \times w_1$  on the cavity wall where  $x = 0$  with the number of holes  $M_1 \times N_1$ , while inner aperture array has a dimension  $l_2 \times w_2$  on the inner cavity wall where  $x = x_1$  with the number of holes  $M_2 \times N_2$ . Point  $P$  is at the center of the enclosure of the cavity where  $x = x_1 + x_2$ .

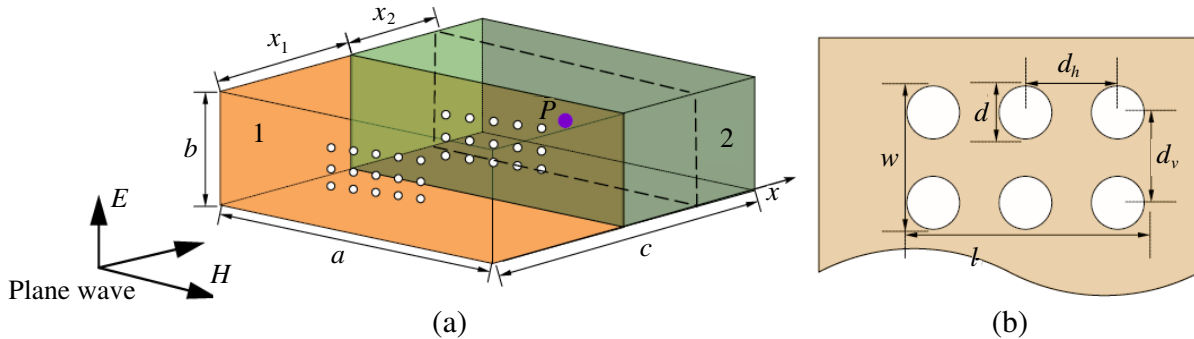


**Figure 1.** The configuration of the dual-cavity structure with an aperture array (a) the dual-cavity structure is  $a$  in length,  $b$  in height,  $c$  in width, the cavity 1 and cavity 2 are  $x_1$  and  $c - x_1$  in width respectively. Point  $P$  is at the center of the enclosure of the cavity where  $x = x_1 + x_2$ . (b) The aperture array is  $l$  in length and  $w$  in width on the wall.  $d$  is the holes diameter,  $d_v$  is the and  $d_h$  are the vertical and horizontal hole distance, here  $d_v$  and  $d_h$  are larger than  $d$ .  $M$  and  $N$  are the number of holes in length and height respectively.

### 2.1. The Aperture Array Impedance

Figure 2 shows the equivalent circuit model of the dual-cavity structure with an aperture array. Assuming that the metal casing is composed of an ideal conductor, the electromagnetic waves incident

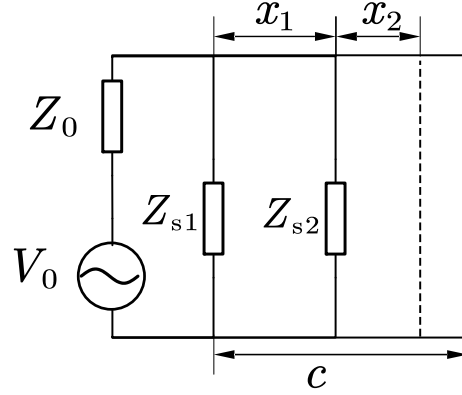


**Figure 2.** The equivalent circuit model of the dual-cavity structure with an aperture array.

on the ideal conductor casing with the array can only enter the casing from the hole array. The incident electromagnetic wave is equivalent to the voltage source  $V_0$ , whose impedance is the wave impedance in free space represented by  $Z_0 = 120\pi \Omega$ .  $Z_{g1}$  and  $Z_{g2}$  are the wave impedances of the outer cavity and inner cavity transmission modes, respectively. For  $TE_{mn}$  mode, the enclosure by the shorted waveguide whose characteristic impedance and propagation constant are  $Z_{gmn} = Z_0 / \sqrt{1 - (m\lambda/2a)^2 - (n\lambda/2b)^2}$  and  $k_{gmn} = k_0 / \sqrt{1 - (m\lambda/2a)^2 - (n\lambda/2b)^2}$ . Here we consider  $TE_{10}$  in which  $m = 1$  and  $n = 0$  for estimating the SE in most simplified situations.

According to the Dehkhoda's model [17, 18], the enclosure of cavity and the aperture array are represented by a short-circuited waveguide and admittance, respectively. The shunt admittance  $Y_{ap}$  of aperture array in a metallic infinite flat plate as showed in Figure 1(b) is

$$Y_{ap}/Y_0 = -j \frac{3d_h d_v \lambda_0}{\pi d^2} + j \frac{288}{\pi \lambda_0 d^2} \left[ \sum_{m=0}^{\infty} \sum_{n=0}^{\infty} \left( \frac{\varepsilon_n^2}{d_v^2} + \frac{\varepsilon_n m^2}{d_h^2} \right) J_1^2(x) \right] \quad (1)$$

where  $\lambda_0$  is the free-space wavelength,  $Y_0$  the intrinsic admittance in the space,  $d$  the holes diameter, and  $d_v$  and  $d_h$  are the vertical and horizontal distances of holes, respectively. Here assuming that both  $d_v$  and  $d_h$  are larger than  $d$ .  $J_1(x)$  is the Bessel functions. The second term in the right side of Equation (1) can be ignored under circumstance that  $d_v$ ,  $d_h$ , and  $d$  of the holes are much less than the wavelength. In this way, the impedance of aperture array in an infinite flat plate could be represented by  $Z_{ap} = 1/Y_{ap}$ , and the aperture array impedance in the finite large cavity shown in Figure 1(b) is obtained by Equation (2)

$$Z_s = Z_{ap} \frac{l \times w}{a \times b} \quad (2)$$

Thus, the outer aperture array impedance  $Z_{s1}$  and the inner aperture array impedance  $Z_{s2}$  can be calculated as follows,

$$\begin{cases} Z_{s1} = Z_{ap} \frac{l_1 \times w_1}{a \times b} \\ Z_{s2} = Z_{ap} \frac{l_2 \times w_2}{a \times b} \end{cases} \quad (3)$$

## 2.2. Electric Shielding Effectiveness

For outer cavity which is region 1 in Figure 1(a), the equivalent voltage  $V_1$  and impedance  $Z_1$  at the first layer hole array are obtained by Thevenin's theory.

$$\begin{cases} V_1 = \frac{Z_{s1} V_0}{Z_{s1} + Z_0} \\ Z_1 = \frac{Z_0 Z_{s1}}{Z_0 + Z_{s1}} \end{cases} \quad (4)$$

Then due to the TML theory, the voltage and impedance at the left end of the inner cavity array can be represented by Equation (5).

$$\begin{cases} V_L = \frac{V_1}{\cos(k_g x_1) + j \frac{Z_1}{Z_g} \sin(k_g x_1)} \\ Z_L = \frac{Z_1 + j Z_g \tan(k_g x_1)}{1 + j \frac{Z_1}{Z_g} \tan(k_g x_1)} \end{cases} \quad (5)$$

Similarly, the equivalent voltage and equivalent impedance at the second layer hole array are

$$\begin{cases} V_2 = \frac{Z_{s2} V_L}{Z_L + Z_{s2}} \\ Z_2 = \frac{Z_L Z_{s2}}{Z_L + Z_{s2}} \end{cases} \quad (6)$$

Hence the equivalent voltage and equivalent impedance at the left of point  $P$  are

$$\begin{cases} V_3 = \frac{V_2}{\cos(k_g x_2) + j \frac{Z_2}{Z_g} \sin(k_g x_2)} \\ Z_3 = \frac{Z_2 + j Z_g \tan(k_g x_2)}{1 + j \frac{Z_2}{Z_g} \tan(k_g x_2)} \end{cases} \quad (7)$$

The impedance of the right wall of the inner cavity is equivalent to the right of point  $P$  as

$$Z_4 = j Z_g \tan[k_g(c - x_1 - x_2)] \quad (8)$$

Finally, the voltage at point  $P$  is obtained by Thevenin's theory.

$$V_P = \frac{V_3 Z_4}{Z_3 + Z_4} \quad (9)$$

Moreover, the load impedance at point  $P$  is  $Z_0$ , and the equivalent voltage at point  $P$  is  $V'_P = \frac{V_0}{2}$  in the absence of the cavity. Therefore, the electric shielding effectiveness is given by

$$SE_e = 20 \lg \left| \frac{V'_P}{V_P} \right| = 20 \lg \left| \frac{V_0}{2V_P} \right| \quad (10)$$

### 3. MODEL VALIDATION AND DISCUSSION

In order to illustrate the validity and accuracy of the presented hybrid model, we compare the results computed by our model with that calculated by the simulation software CST. In the comparisons, some typical examples are considered. The rectangular dual-cavity structure with a circle aperture array used is shown in Figure 1, where  $a = c = 300$  mm,  $b = 120$  mm, all wall thickness  $t$  is 1 mm. Other dimensional parameters of the typical dual-cavity structure are given in Table 1. The frequency band is between 0 Hz and 1 GHz because most EMI always needs shielding in this range practically. The monitor probe  $P$  is at the center of the enclosure just for validating the accuracy of the hybrid model.

The electric SE for example 1 is shown in Figure 3(a), together with the result calculated by CST. The observation point  $P$  is the center of the enclosure of the cavity, at a height 60 mm and a width 150 mm. The number of holes is  $5 \times 3$  in both the outer array and the inner array. The holes diameter is 10 mm, while the vertical and horizontal hole separations are both 20 mm. It can be observed that the result of the hybrid model is in good agreement with CST simulation ones. It indicates that the resonant frequency is about 909 MHz. The tendency of the analytical results is consistent with simulation ones. The result of example 1 could be a comparison standard with other examples.

**Table 1.** Typical examples of the dual-cavity structure with an aperture array considered.

Examples	$x_1$ (mm)	$x_2$ (mm)	$M_1$	$N_1$	$M_2$	$N_2$	$d$ (mm)	$d_v$ (mm)	$d_h$ (mm)
1	100	50	5	3	5	3	10	20	20
2	100	50	5	3	5	3	5	10	10
3	100	50	10	6	5	3	10	20	20
4	150	50	5	3	5	3	10	20	20

Compared with example 1, example 2 changes the holes diameter and holes separations. The result is shown in Figure 3(b), and the SE becomes larger than example 1 due to the diminishing holes diameter. Figure 3(c) indicates that the SE gets smaller than example 1 due to the increased number of elements in array 1. The resonant frequencies of example 2 and example 3 are also about 909 MHz since the size of cavity is unchanged. Figure 3(d) presents the resonant frequency at about 1124 MHz, where  $x = 200$  mm in example 4. It can be seen that the size of the cavity changed the resonate frequency. From Figure 3(a) to Figure 3(d), the hybrid model can predict the first resonance point and the tendency of SE. Clearly the hybrid model is accurate in this range of frequencies, where TE<sub>10</sub> mode is dominant.

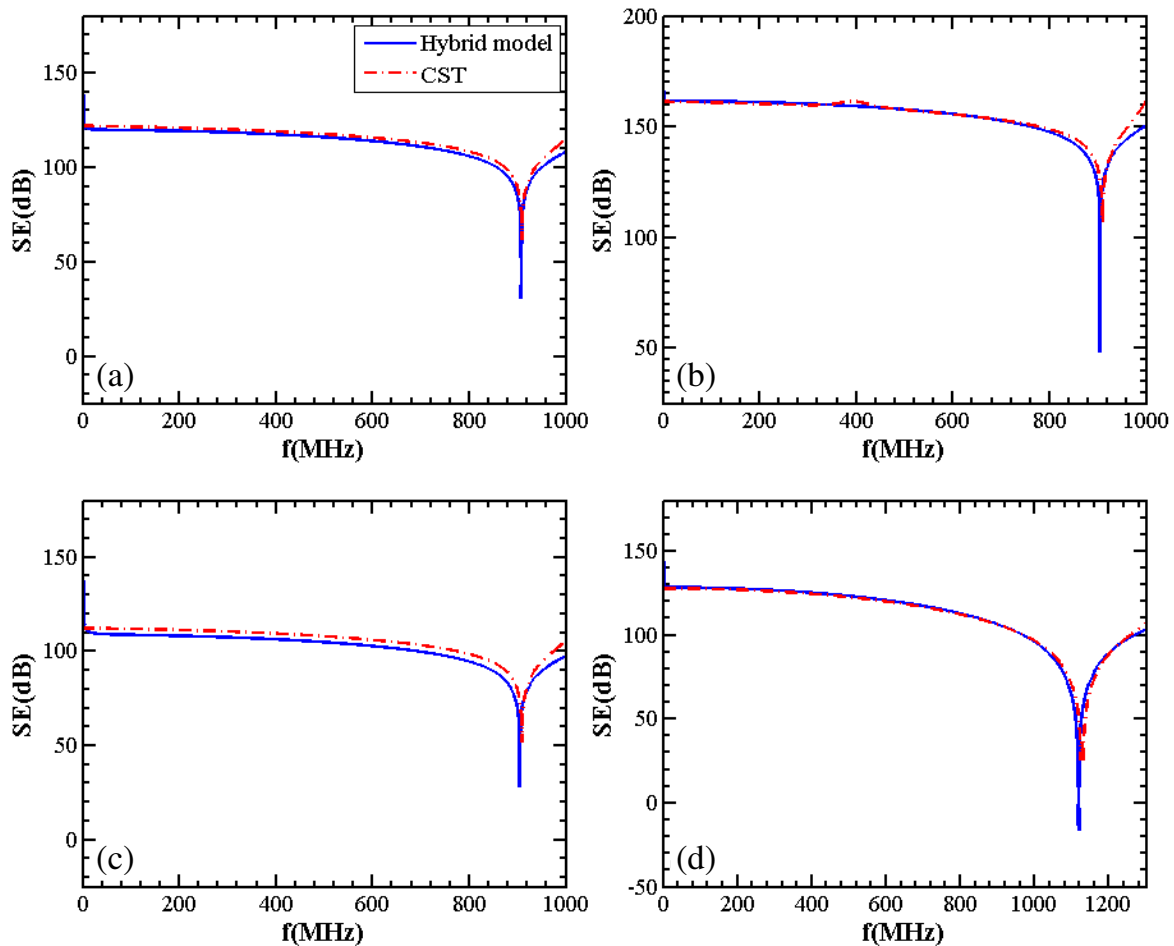


**Figure 3.** Electric SE for (a) example 1, (b) example 2, (c) example 3, (d) example 4. Continuous line: Hybrid model simulation. Dashed line: CST simulation.

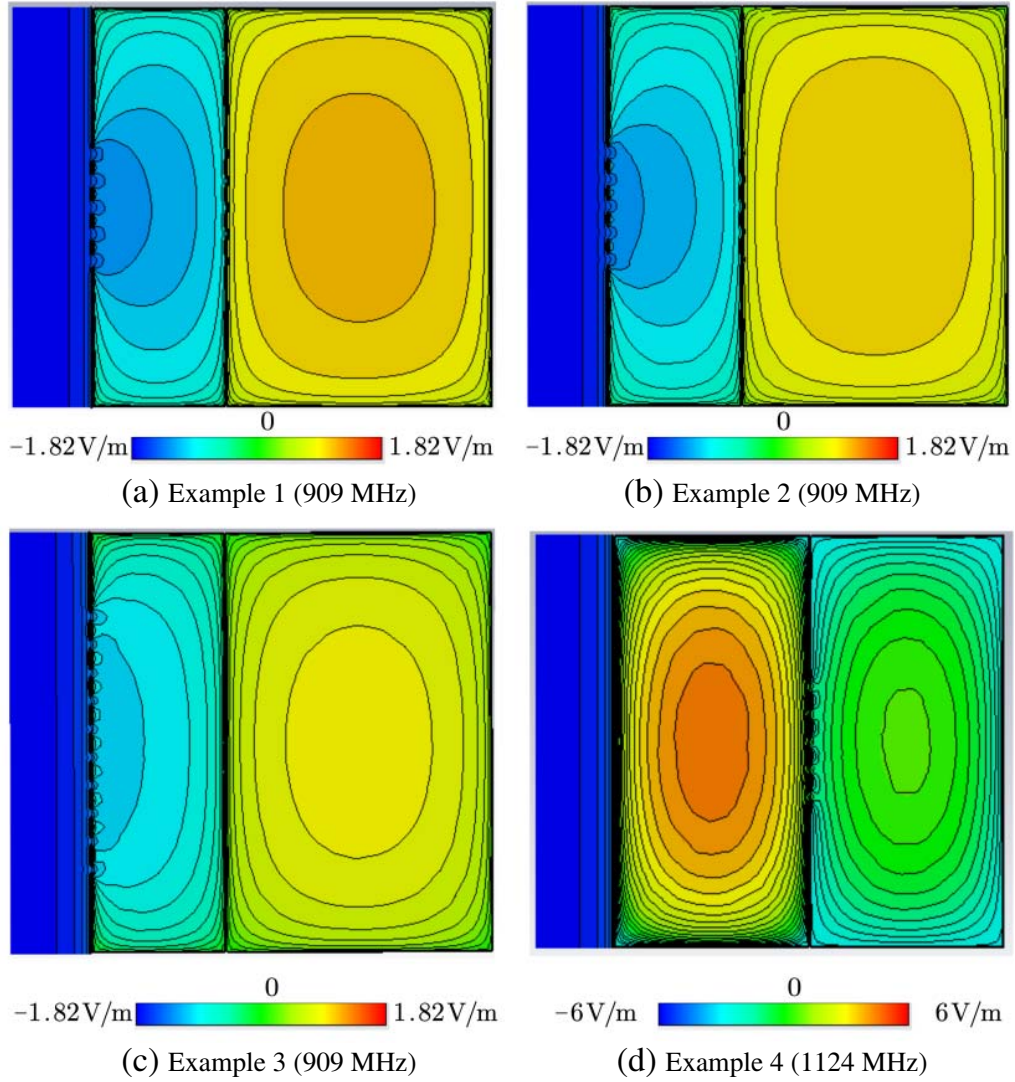


**Figure 4.** Field distribution of the dual-cavity structure for (a) example 1, (b) example 2, (c) example 3, (d) example 4 under resonant frequencies, where  $TE_{10}$  mode is dominate.

The extreme point of the field strength distribution is exactly at the center point of the inner cavity, as shown in Figure 4(a)~Figure 4(d). Although the field strength distribution in the cavity is different at different resonant frequencies for different examples, the extreme point of the field strength distribution is always at the center of the inner cavity. According to the calculations, in the frequency range of 0–1.5 GHz, these examples have two resonant frequencies that totally meet the above conditions, where  $TE_{10}$  mode is dominant. It matches the results of this paper and proves the correctness of our analytical hybrid model once again.

In these results, however, there is a little difference between the presented model and the CST simulation above the first resonance frequency. One possible reason is that the aperture array is regarded as an admittance, it might bring errors into results. The other reason is that this model only considers the dominant  $TE_{10}$  mode in the enclosure, but other modes exist at higher frequencies, and it may also lead to some difference. For instance, the array will strongly excite the  $TE_{11}$  and  $TM_{11}$  modes, and these modes will be present at frequencies above first resonant frequency.

#### 4. CONCLUSIONS

In this paper, an analytical hybrid model based on Robinson's model and Dehkhoda's model is proposed. Assuming that the enclosure of a dual-cavity structure is equivalent to a short-circuited waveguide, and the aperture array is regarded as an impedance. Then the analytical solution is obtained through Thevenin's theory and TML theory. It is demonstrated that the results of this hybrid model have a good agreement with CST simulation in typical examples under the dominant  $TE_{10}$  mode. This hybrid analytical model provides a fast way to get an analytic solution on the desk for designers to speed up the design process of a dual-cavity structure with an aperture array, especially where the accuracy is not required strictly.

Research on extending this analytical hybrid model in high TE mode and TM mode for more accuracy solution is conducted as a next step.

#### ACKNOWLEDGMENT

This work is supported by the National Natural Science Foundation of China, grant number 61801201, the Basic Research Project of National Defense Science and Technology of China, grant number JCKY2018203B030, and the Foundation of Key Laboratory of Gansu Advanced Control for Industrial Processes, grant number XJ201804 and XJ201808.

#### REFERENCES

1. Araneo, R. and G. Lovat, "Fast MoM analysis of the shielding effectiveness of rectangular enclosures with apertures, metal plates, and conducting objects," *IEEE Transactions on Electromagnetic Compatibility*, Vol. 51, No. 2, 274–283, 2009.
2. Nie, B.-L., P.-A. Du, Y.-T. Yu, and Z. Shi, "Study of the shielding properties of enclosures with apertures at higher frequencies using the transmission-line modeling method," *IEEE Transactions on Electromagnetic Compatibility*, Vol. 53, No. 1, 73–81, 2010.
3. Georgakopoulos, S. V., C. R. Birtcher, and C. A. Balanis, "HIRF penetration through apertures: FDTD versus measurements," *IEEE Transactions on Electromagnetic Compatibility*, Vol. 43, No. 3, 282–294, 2001.
4. Tesche, F. M., "Topological concepts for internal EMP interaction," *IEEE Transactions on Electromagnetic Compatibility*, Vol. 1, 60–64, 1978.
5. Baum, C. E., T. K. Liu, and F. M. Tesche, "On the analysis of general multiconductor transmission-line networks," *Interaction Note*, Vol. 350, No. 6, 467–547, 1978.
6. Baum, C. E., "Including apertures and cavities in the BLT formalism," *Electromagnetics*, Vol. 25, Nos. 7–8, 623–635, 2005.
7. Kan, Y., L.-P. Yan, X. Zhao, H.-J. Zhou, Q. Liu, and K.-M. Huang, "Electromagnetic topology based fast algorithm for shielding effectiveness estimation of multiple enclosures with apertures," *Acta Physica Sinica*, Vol. 65, No. 3, 030702, 2016.
8. Nie, B.-L. and P.-A. Du, "Electromagnetic shielding performance of highly resonant enclosures by a combination of the FETD and extended Prony's method," *IEEE Transactions on Electromagnetic Compatibility*, Vol. 56, No. 2, 320–327, 2013.
9. Kuo, C.-W. and C.-M. Kuo, "Finite-difference time-domain analysis of the shielding effectiveness of metallic enclosures with apertures using a novel subgridding algorithm," *IEEE Transactions on Electromagnetic Compatibility*, Vol. 58, No. 5, 1595–1601, 2016.
10. Basyigit, I. B., H. Dogan, and S. Helhel, "Simulation of metallic enclosures with apertures on electrical shielding effectiveness," *2017 10th International Conference on Electrical and Electronics Engineering (ELECO)*, 1082–1084, IEEE, 2017.
11. Bethe, H. A., "Theory of diffraction by small holes," *Physical Review*, Vol. 66, Nos. 7–8, 163, 1944.

12. Robinson, M. P., J. Turner, D. W. Thomas, J. Dawson, M. Ganley, A. Marvin, S. Porter, T. Benson, and C. Christopoulos, "Shielding effectiveness of a rectangular enclosure with a rectangular aperture," *Electronics Letters*, Vol. 32, No. 17, 1559–1560, 1996.
13. Robinson, M. P., T. M. Benson, C. Christopoulos, J. F. Dawson, M. Ganley, A. Marvin, S. Porter, and D. W. Thomas, "Analytical formulation for the shielding effectiveness of enclosures with apertures," *IEEE Transactions on Electromagnetic Compatibility*, Vol. 40, No. 3, 240–248, 1998.
14. Thomas, D. W., A. C. Denton, T. Konefal, T. Benson, C. Christopoulos, J. Dawson, A. Marvin, S. J. Porter, and P. Sewell, "Model of the electromagnetic fields inside a cuboidal enclosure populated with conducting planes or printed circuit boards," *IEEE Transactions on Electromagnetic Compatibility*, Vol. 43, No. 2, 161–169, 2001.
15. Konefal, T., J. Dawson, and A. Marvin, "Improved aperture model for shielding prediction," *2003 IEEE Symposium on Electromagnetic Compatibility*, 187–192, Symposium Record (Cat. No. 03CH37446), IEEE, 2003.
16. Dan, S., Y. Shen, and Y. Gao, "3 high-order mode transmission line model of enclosure with off-center aperture," *2007 International Symposium on Electromagnetic Compatibility*, 361–364, IEEE, 2007.
17. Dehkhoda, P., A. Tavakoli, and R. Moini, "An efficient and reliable shielding effectiveness evaluation of a rectangular enclosure with numerous apertures," *IEEE Transactions on Electromagnetic Compatibility*, Vol. 50, No. 1, 208–212, 2008.
18. Dehkhoda, P., A. Tavakoli, and R. Moini, "Fast calculation of the shielding effectiveness for a rectangular enclosure of finite wall thickness and with numerous small apertures," *Progress In Electromagnetics Research*, Vol. 86, 341–355, 2008.
19. Ren, D., P.-A. Du, Y. He, K. Chen, J.-W. Luo, and D. G. Michelson, "A fast calculation approach for the shielding effectiveness of an enclosure with numerous small apertures," *IEEE Transactions on Electromagnetic Compatibility*, Vol. 58, No. 4, 1033–1041, 2016.
20. Lee, J. G., H. J. Eom, B. W. Kim, and H. H. Park, "Shielding effectiveness of enclosure with thick multiple apertures," *Microwave and Optical Technology Letters*, Vol. 29, No. 3, 178–181, 2001.
21. Nie, B.-L., P.-A. Du, and P. Xiao, "An improved circuital method for the prediction of shielding effectiveness of an enclosure with apertures excited by a plane wave," *IEEE Transactions on Electromagnetic Compatibility*, Vol. 60, No. 5, 1376–1383, 2017.
22. Hu, P.-Y. and X. Sun, "Study of the calculation method of shielding effectiveness of rectangle enclosure with an electrically large aperture," *Progress In Electromagnetics Research M*, Vol. 61, 85–96, 2017.